

## Supplementary Information

# Exquisite Sequence Selectivity with Small Conditional RNAs

Jonathan B. Sternberg<sup>1</sup> and Niles A. Pierce<sup>1,2,\*</sup>

<sup>1</sup>Division of Biology & Biological Engineering, <sup>2</sup>Division of Engineering & Applied Science,  
California Institute of Technology, Pasadena, CA 91125, USA

\*Email: [niles@caltech.edu](mailto:niles@caltech.edu)

# Contents

<b>S1 Materials and methods</b>	<b>S3</b>
S1.1 Oligonucleotide sequences . . . . .	S3
S1.2 Oligonucleotide synthesis and purification . . . . .	S3
S1.3 Reaction conditions . . . . .	S3
S1.4 Polyacrylamide gel electrophoresis . . . . .	S4
<b>S2 Discrimination of RNA SBS cancer markers and wildtype sequences</b>	<b>S7</b>
S2.1 Annotated single-channel scans for the gels in Figure 3 . . . . .	S7
S2.2 Further characterization of the scRNAs used in Figure 3 . . . . .	S7
S2.3 Quantification of ON/OFF ratios . . . . .	S7
<b>S3 Enhancing selectivity via competitive inhibition with an unstructured scavenger</b>	<b>S12</b>
S3.1 Further characterization of the scRNAs and scavenger used in Figure 4 . . . . .	S12
S3.2 Scavenger studies with additional SNPs . . . . .	S12
<b>S4 Genotyping SNPs</b>	<b>S13</b>
S4.1 Annotated single-channel scans for the gel in Figure 5 . . . . .	S13
<b>S5 Additional studies</b>	<b>S14</b>
S5.1 Effect of SBS mutation location on scRNA selectivity . . . . .	S14
S5.2 Effect of temperature on scRNA selectivity . . . . .	S15

# S1 Materials and methods

## S1.1 Oligonucleotide sequences

Each family of 18–36-nt RNA targets comprises two or more 1-nt sequence variants differing by an SBS mutation or an SNP; for each target, the cognate h1 scRNA recognizes an 18–20-nt marker (a subsequence of the target) containing the mutation or polymorphism. Each HCR scRNA has a 4-nt toehold, a 14–16-bp stem, and a 4-nt hairpin loop. With the exception of the loop of the h1 scRNA and the complementary toehold of the h2 scRNA, the sequences are fully determined by the sequence of the marker (which is identical in sequence to the output domain of h2). Hence, the majority of the sequence is designed by setting the register of h1 relative to the target. We optimized the timing of sequence selectivity for a timescale of choice by adjusting toehold strength for each of the two scRNAs relative to the toehold strength of previously tested scRNAs. Free energy calculations were performed using the Analysis page of the NUPACK web application.<sup>1</sup> Increasing the energetic driving force for polymerization leads to selectivity at an earlier time point; decreasing the energetic driving force for polymerization leads to selectivity at a later time point. In cases where spontaneous polymerization was too rapid, we increased the stem length of the scRNAs to increase the strength of kinetic trapping.<sup>2</sup> It can be useful to purposely include one or more wobble pairs or mismatches between h1 and the target in order to reduce their affinity, in which case the target no longer fully determines the sequence of the input domain for h1. In this study, H<sup>U</sup> of Figure 5 employs an h1 scRNA that forms a wobble pair with cognate target X<sup>A</sup> (but a Watson–Crick pair with h2), and H<sup>C</sup> of Figure S5b employs an h1 scRNA that forms a wobble pair with cognate target X<sup>G</sup> (as well as with h2). Each 11–12-nt scavenger was designed by adjusting the register and length of the scavenger in order to tune the predicted free energy of hybridization with the target relative to that of previously tested scavengers. Sequences for RNA targets are shown in Table S1. Sequences for RNA scavengers are shown in Table S2. Sequences for scRNAs are shown in Table S3.

## S1.2 Oligonucleotide synthesis and purification

Targets, scRNAs, and scavengers were synthesized by Integrated DNA Technologies (IDT). Oligonucleotides were resuspended in ultrapure water (Corning, Cat. # 46-000-CM) in our lab. Fluorescent scRNAs were ordered from IDT end-labeled either with a fluorophore or with an amine to permit subsequent coupling of a fluorophore. Dye coupling reactions were performed as follows: to label h2 of HCR system H<sup>C</sup> with Cy5, we combined 28  $\mu\text{L}$  of sodium tetraborate decahydrate (0.1 M, pH 8.5), 4.1  $\mu\text{L}$  of amine-labeled scRNA in ultrapure water (1.5  $\mu\text{M}$ ), and 5.25  $\mu\text{L}$  of Cy5 in DMSO (18  $\mu\text{g}/\mu\text{L}$ ; GE Healthcare, Cat. # PA25001), mixing every 30 min for two hours and incubating in the dark at room temperature overnight; to label h1 of HCR system H<sup>U</sup> with Alexa488, the same procedure was used except that the dye was used in its entirety (Life Technologies, Cat. # A32761); to label h2 of HCR system H<sup>C</sup> with Alexa488, we combined 1.75  $\mu\text{L}$  of 10 $\times$  conjugation buffer (0.5 M Na<sub>2</sub>HPO<sub>4</sub>, 10 mM EDTA, pH 8.5), 10  $\mu\text{L}$  of amine-labeled scRNA in ultrapure water (250  $\mu\text{M}$ ), and 5.25  $\mu\text{L}$  of DMSO containing the full sample of Alexa488 (Life Technologies, Cat. # A32761).

Oligonucleotides were typically HPLC-purified by IDT. Otherwise, they were desalted by IDT and then purified using a 10% or 15% denaturing polyacrylamide gel. The band corresponding to the expected mobility was visualized by UV shadowing and excised from the gel. Oligonucleotides were then eluted by soaking in 0.3 M NaCl overnight and recovered by ethanol precipitation. After dye coupling reactions, scRNAs were purified from unincorporated dyes by ethanol precipitation and then resuspended in ultrapure water. Fluophore-labeled scRNAs were then purified from unlabeled scRNAs using the above strand purification procedure.

## S1.3 Reaction conditions

Oligonucleotides were stored at  $-20\text{ }^\circ\text{C}$ , brought to room temperature on the bench top, and quantified in  $1 \times$  PKR buffer (20 mM HEPES pH 7.5, 4 mM MgCl<sub>2</sub>, 100 mM KCl) by measuring absorbance at 260 nm. Prior to use, each oligonucleotide was snap-cooled (heat at  $95\text{ }^\circ\text{C}$  for 90 s followed by incubation on ice for 30 s and incubation at room temperature for a minimum of 15 min) at a convenient concentration ranging from 2 to 40  $\mu\text{M}$ ; snap-cooling is helpful in ensuring that h1 and h2 predominantly form hairpin monomers prior to the start of each HCR reaction.

For reactions that contained multiple HCR systems, a master mix of the relevant scRNAs was created, adding all h1 scRNAs to the test tube, then expelling all h2 scRNAs onto the walls of the test tube, and finally mixing all scRNAs together. This procedure enabled the h1 and h2 scRNAs for each HCR system to be mixed at their diluted master mix concentrations to minimize spontaneous polymerization. In reactions that contained scavengers, targets were first introduced to the bottom of the reaction test tubes and then scavengers and scRNAs were expelled onto opposite sides of the test tube walls and mixed in together, providing scavengers and scRNAs simultaneous access to the targets.

Reactions were typically carried out with targets and scRNAs at 1  $\mu$ M (scavengers at 2  $\mu$ M, when applicable) in 1  $\times$  PKR at 37  $^{\circ}$ C for 1 h. Reaction volumes ranged from 5 to 30  $\mu$ L, with larger volumes favored for long reactions in order to minimize the influence of evaporation effects over the course of the experiment. To move the selectivity window earlier in time, scRNAs were used at 2  $\mu$ M for certain systems (for the BRAF wildtype-detecting system H<sup>A</sup> of Figures 3a, S1a, S2a and S3a and the SNP-detecting systems H<sup>C</sup> and H<sup>G</sup> of Figures 5 and S6). All targets for the SNP studies of Figures 5 and S6 were also introduced at 2  $\mu$ M. Reactions for the mutant- and wildtype-detecting BRAF systems of Figures 3a, S1a, S2a and S3a were carried out for 2 h. Multiple time points were tested for the kinetic discrimination study of Figure 2, the mutation location study of Figure S7, and the temperature study of Figure S8 (which also tested multiple temperatures). Reactions for the temperature study were performed in the cold room.

#### **S1.4 Polyacrylamide gel electrophoresis**

Following HCR reactions, 5  $\times$  loading buffer (50% glycerol, 1  $\times$  PKR) was added directly to the reaction test tubes or to a fraction of the reaction mixture placed in a new test tube. Typically, 3  $\mu$ L of this mixture was loaded into individual gel lanes. For the fluorophore-labeled mutant- and wildtype-detecting BRAF systems of Figures 3a, S1a, S2a and S3a, only 1.5  $\mu$ L was loaded into gel lanes. Typically, 15-lane 10% native TBE gels (Bio-Rad, Cat. # 456-1036S) were run at 150 V for 42 min at room temperature. Gels for the temperature study of Figure S8 were run in the cold room. For the quantification studies of Figure S3, gels were run at 150 V for 21 min at room temperature. Gels were imaged on an FLA-5100 laser scanner (FujiFilm). Gels not containing fluorescently-labeled hairpins were post-stained with SYBR Gold (Invitrogen Cat. # S-11494) and imaged with a 473 nm laser and a 530  $\pm$  10 nm band-pass filter. Gels containing fluorescently-labeled hairpins were imaged using appropriate excitation lasers and emission filters (Alexa488: 473 nm/530  $\pm$ 10 nm, Cy3: 532 nm/570  $\pm$ 10 nm, Cy5 and Alexa647: 635 nm/665 nm long-pass filter). The 4-channel gel of Figures 5 and S6 was imaged with the above three channels on the FLA-5100 and then imaged on an Odyssey imaging system (Li-Cor) for the fourth channel (Alexa750: 785 nm/810 nm long-pass filter). Scans from the two instruments were then merged using the TurboReg plugin of ImageJ.

**Table S1. RNA target sequences.** Sequence variants in orange.

Name	# (nt)	Sequence (5' to 3')	Figures
X	36	GAUUUUGGUCUAGCUACAGAGAAAUCUCGAUGGAGU	2, S8
X'	36	GAUUUUGGUCUAGCUACAGUGAAAUCUCGAUGGAGU	2, S8
X''	36	GAUUUUGGUCUAGCAACAGUGAAAUCUCGAUGGAGU	2
X <sup>A</sup>	36	GAUUUUGGUCUAGCUACAGAGAAAUCUCGAUGGAGU	3a, S1a, S2a, S3a
X <sup>U</sup>	36	GAUUUUGGUCUAGCUACAGUGAAAUCUCGAUGGAGU	3a, S1a, S2a, S3a
X <sup>U</sup>	36	UUGGUUUUAAAUAUGGAGUAUGUUUCUGUGGAGAC	3b, S1b, S2b, S3b, S5b
X <sup>G</sup>	36	UUGGUUUUAAAUAUGGAGUAUGUGUCUGUGGAGAC	3b, S1b, S2b, S3b, S5b
X <sup>G</sup>	36	CUGUAAAGCUGGAAAGGGAGGAACUGGUGUAAUGAU	3c, 5, S1c, S2c, S3c, S6
X <sup>C</sup>	36	CUGUAAAGCUGGAAAGGGACGAACUGGUGUAAUGAU	3c, 5, S1c, S2c, S3c, S6
X <sup>A</sup>	26	GAUUUUGGUCUAGCUACAGAGAAAUC	4, S4, S5a
X <sup>G</sup>	26	GAUUUUGGUCUAGCUACAGGGAAAUC	4, S4, S5a
X <sup>C</sup>	26	GAUUUUGGUCUAGCUACAGCGAAAUC	S5a
X <sup>U</sup>	26	GAUUUUGGUCUAGCUACAGUGAAAUC	S5a
X <sup>A</sup>	36	UUGGUUUUAAAUAUGGAGUAUGUAUCUGUGGAGAC	S5b
X <sup>C</sup>	36	UUGGUUUUAAAUAUGGAGUAUGUCUCUGUGGAGAC	S5b
X <sup>A</sup>	26	CUGUAAAGCUGGAAAGGGAAGAACUG	S5c
X <sup>C</sup>	26	CUGUAAAGCUGGAAAGGGACGAACUG	S5c
X <sup>G</sup>	26	CUGUAAAGCUGGAAAGGGAGGAACUG	S5c
X <sup>U</sup>	26	CUGUAAAGCUGGAAAGGGAUGAACUG	S5c
X <sup>A</sup>	36	CUGUAAAGCUGGAAAGGGAAGAACUGGUGUAAUGAU	5, S6
X <sup>U</sup>	36	CUGUAAAGCUGGAAAGGGAUGAACUGGUGUAAUGAU	5, S6
X	18	CACACACCACACCACACG	S7ab
M1	18	CAGACACCACACCACACG	S7a
M2	18	CACAGACCACACCACACG	S7a
M3	18	CACACACCAGACCACACG	S7a
M4	18	CACACACCACACCAGACG	S7a
M1	18	CAUACACCACACCACACG	S7b
M2	18	CACAUACCACACCACACG	S7b
M3	18	CACACACCAUACCACACG	S7b
M4	18	CACACACCACACCAUACG	S7b
X	18	UGACCUGACUUGACUGAC	S7cd
M1	18	UGACCUGACUUGACUUAC	S7c
M2	18	UGACCUGACUUUACUGAC	S7c
M3	18	UGACCUUACUUGACUGAC	S7c
M4	18	UUACCUGACUUGACUGAC	S7c
M1	18	UGACCUGACUUGACUAAAC	S7d
M2	18	UGACCUGACUUUACUGAC	S7d
M3	18	UGACCUAAACUUGACUGAC	S7d
M4	18	UAACCUGACUUGACUGAC	S7d

**Table S2. Scavenger sequences.** Nucleotides complementary to target sequence variants in blue.

Name	# (nt)	Sequence (5' to 3')	Figures
S <sup>C</sup>	11	UUUC <u>CC</u> UGUAG	4, S4, S5a
S <sup>A</sup>	12	AUUUC <u>AC</u> UGUAG	S5a
S <sup>U</sup>	12	AUUUC <u>UC</u> UGUAG	S5a
S <sup>C</sup>	11	CAGAC <u>CA</u> UAUC	S5b
S <sup>U</sup>	12	ACAGA <u>UA</u> CAUAC	S5b

**Table S3. scRNA sequences.** Nucleotides complementary to target sequence variants in lavender; toehold nucleotides are underlined.

Name	# (nt)	Sequence (5' to 3')	Figures
H <sup>fast</sup> (h1)	36	CAGAGAAAUCUCGACAGAUCCGAGAUUUUCUGUAGC	2, S8
H <sup>fast</sup> (h2)	36	<u>UCUCGAGAUUUUCUGGCUACAGAGAAAUCUCGA</u>	2, S8
H <sup>medium</sup> (h1)	36	<u>UCUCUGUAGCUGAGACCAACAAAUUGGUCUAGCUACA</u>	2, S8
H <sup>medium</sup> (h2)	36	<u>UUGGUCUAGCUACAGAGUAGUAGCUAGACCAAUUUG</u>	2, S8
H <sup>slow</sup> (h1)	36	<u>GAUUUCUCUGUAGCUGAGACUUCUAGCUACAGAGA</u>	2, S8
H <sup>slow</sup> (h2)	36	<u>UCUAGCUACAGAGAAAUCUCUGUAGCUAGAAGUC</u>	2, S8
H <sup>U</sup> (h1) BRAF	40	<u>UACAGAGAAAUCUCGGAAGAUCGAGAUUUUCUGUAGCUA</u>	3a, S1a, S2a, S3a
H <sup>U</sup> (h2) BRAF	40	<u>AUCUUCGAGAUUUUCUCUGUUAUCGACAGAGAAAUCUCGA</u> / iSp9 // 3Cy3Sp /	3a, S1a, S2a, S3a
H <sup>A</sup> (h1) BRAF	38	<u>UCUCUGUAGCUGAGACCAAAUAGUUUUGGUCUAGCUACA</u>	3a, S1a, S2a, S3a
H <sup>A</sup> (h2) BRAF	38	<u>UUUGGUCUAGCUACAGUAGUAGUAGCAGACCAAAACUA</u> / iSp9 // 3Cy5Sp /	3a, S1a, S2a, S3a
H <sup>A</sup> (h1) JAK2	36	<u>UCCACAGAAACAUAUCUCUCUUGGAGUAUGUUUCUG</u>	3b, S1b, S2b, S3b
H <sup>A</sup> (h2) JAK2	36	<u>/ 5A1ex647N // iSp9 / GGAGUAUUGUUCUGUGGACAGAAAACAUAUCUCCAAGA</u>	3b, S1b, S2b, S3b
H <sup>C</sup> (h1) JAK2	38	<u>GUAUGUGUCUGUGGAAAGAAUCCACAGACACAUACUCCA</u>	3b, S1b, S2b, S3b
H <sup>C</sup> (h2) JAK2	38	<u>UUCUCCACAGACACAUAUCUGGAGUAUGUCUGUGGA</u> / iSp9 // 3AmMO / (Alexa488)	3b, S1b, S2b, S3b
H <sup>C</sup> (h1) PTEN	36	<u>GAGGAACUGGUGUAAACAUAACACAGUUCUUCUUCU</u>	3c, 5, S1c, S2c, S3c, S6
H <sup>C</sup> (h2) PTEN	36	<u>UGUUACACACAGUUCUCCAGGGAGAACUGGUGUA</u> / iSp9 // 3AmMO / (Cy5)	3c, 5, S1c, S2c, S3c, S6
H <sup>G</sup> (h1) PTEN	36	<u>CAGUUCGUCCUUCACAGGAAACUGGAAAGGACGA</u> / iSp9 // 3Cy3Sp /	3c, 5, S1c, S2c, S3c, S6
H <sup>G</sup> (h2) PTEN	36	<u>CUGGAAAAGGACGAAACUGUCGUCCUUCUCCAGUUUC</u>	3c, 5, S1c, S2c, S3c, S6
H <sup>U</sup> (h1)	36	<u>UCUCUGUAGCUAGACCAACAAAUUGGUCUAGCUACA</u>	4, S4, S5a
H <sup>U</sup> (h2)	36	<u>UUGGUCUAGCUACAGAGUAGUAGCUAGACCAAUUUG</u>	4, S4, S5a
H <sup>A</sup> (h1)	36	<u>UCACUGUAGCUAGACCAACAAAUUGGUCUAGCUACA</u>	S5a
H <sup>A</sup> (h2)	36	<u>UUGGUCUAGCUACAGUAGUAGCUAGACCAAUUUG</u>	S5a
H <sup>A</sup> (h1)	36	<u>UCCAAGAAACAUAUCUCCUUCUUGGAGUAUGUUUCUG</u>	S5b
H <sup>A</sup> (h2)	36	<u>GGAGUAUGUUUCUGUGGACAGACAAACAUAUCUCCAAGA</u>	S5b
H <sup>C</sup> (h1)	38	<u>GUAUGUUCUGUGGAAAGAAUCCACAGACACAUACUCUA</u>	S5b
H <sup>C</sup> (h2)	38	<u>UUCUCCACAGACACAUAUCUGGAGUAUGUCUGUGGA</u>	S5b
H <sup>C</sup> (h1)	36	<u>CAGUUCUCCUUCUCCAGGAAACUGGAAAGGAGGA</u>	S5c
H <sup>C</sup> (h2)	36	<u>CUGGAAAAGGAGGAAACUGUCCUUCUCCAGUUUC</u>	S5c
H <sup>G</sup> (h1)	36	<u>CAGUUCGUCCUUCACAGGAAACUGGAAAGGACGA</u>	S5c
H <sup>G</sup> (h2)	36	<u>CUGGAAAAGGACGAAACUGUCGUCCUUCUCCAGUUUC</u>	S5c
H <sup>U</sup> (h1)	38	<u>CACUAGUUCUUCUCCUUCUCCAGGAAAGGAAAGAAACU</u> / iSp9 // 3AmMO / (Alexa488)	5, S6
H <sup>U</sup> (h2)	38	<u>GGAAAGGAAAGAAACUAGUGAGUUCUCCUUCUCCUUGA</u>	5, S6
H <sup>A</sup> (h1)	36	<u>/ 5A1ex750N // iSp9 / AAGGAAUGAAUCUGGUAUCUCCAGUUCUCCUUCUCCA</u>	5, S6
H <sup>A</sup> (h2)	36	<u>AUGACCAAGUUCUCCUUCUCCUUGGAAAGGAAAGAAACUGG</u>	5, S6
(h1)	36	<u>CACCACACCACAGGAGACGUGUGGUGUGUGUGUGUG</u>	S7ab
(h2)	36	<u>UCUCCGUGUGUGUGGACACACCAACACACACG</u>	S7ab
(h1)	36	<u>GUCAGUCAAGUCAGGUCAAAGAUAGACCUGACUUGAC</u>	S7cd
(h2)	36	<u>UGACCUGACUUGACUGACGUCAGUACAGGUCUUCUUCU</u>	S7cd

## S2 Discrimination of RNA SBS cancer markers and wildtype sequences

### S2.1 Annotated single-channel scans for the gels in Figure 3

Single-channel scans for the gels in Figure 3 are shown in Figure S1, including an additional lane depicting spontaneous polymerization in the absence of target. Migration of scRNAs, homodimers, and polymers is annotated for each of the six HCR systems. The complementarity of the “b” and “b\*” domains within each h1 and h2 scRNA (see Figure 1) enables formation of off-pathway homodimers in which two h1 or h2 monomers hybridize to each other to form two duplex stems separated by an interior loop. Formation of these minor products is kept to a minimum by snap-cooling each scRNA species prior to the start of an experiment (Section S1.3), kinetically trapping most scRNAs in the desired monomer state.

### S2.2 Further characterization of the scRNAs used in Figure 3

For each of three SBS cancer markers (BRAF, JAK2, PTEN), Figure S2 characterizes the selectivity of mutant-detecting and wildtype-detecting HCR systems. All HCR systems exhibit high selectivity for their cognate target both in test tubes that contain a single HCR system and in test tubes that contain both mutant-detecting and wildtype-detecting HCR systems. In some instances, competitive inhibition between scRNAs enhances selectivity for reactions containing two HCR systems (e.g., for BRAF,  $H^A$  reduces off-target activation of  $H^U$  (lane 3 vs 9 of Figure S2a middle panel) and  $H^U$  reduces off-target activation of  $H^A$  (lane 6 vs 8 of Figure S2a bottom panel)).

### S2.3 Quantification of ON/OFF ratios

For each of three SBS cancer markers (BRAF, JAK2, PTEN), we quantified performance for mutant-detecting and wildtype-detecting HCR systems ( $H_M$  and  $H_{WT}$ ) in test tubes containing both HCR systems labeled with spectrally distinct fluorophores (red channel for  $H_M$ , green channel for  $H_{WT}$ ). Figure S3 shows both channels for each cancer marker; these data represent one of five replicate sets of experiments. For a given replicate, the normalized polymerization is calculated for each combination of HCR system ( $H_M$  and  $H_{WT}$ )\* and target ( $X_M$  and  $X_{WT}$ )†:

$$\begin{aligned} H_M(X_M) &= \frac{1}{2} \left[ \frac{r_2 - \frac{1}{2}(r_1 + r_3)}{r_2^{\text{tot}} - \frac{1}{2}(r_1^{\text{tot}} + r_3^{\text{tot}})} + \frac{r_4 - \frac{1}{2}(r_3 + r_5)}{r_4^{\text{tot}} - \frac{1}{2}(r_3^{\text{tot}} + r_5^{\text{tot}})} \right] \\ H_M(X_{WT}) &= \frac{1}{2} \left[ \frac{r_8 - \frac{1}{2}(r_7 + r_9)}{r_8^{\text{tot}} - \frac{1}{2}(r_7^{\text{tot}} + r_9^{\text{tot}})} + \frac{r_{10} - \frac{1}{2}(r_9 + r_{11})}{r_{10}^{\text{tot}} - \frac{1}{2}(r_9^{\text{tot}} + r_{11}^{\text{tot}})} \right] \\ H_{WT}(X_M) &= \frac{1}{2} \left[ \frac{g_2 - \frac{1}{2}(g_1 + g_3)}{g_2^{\text{tot}} - \frac{1}{2}(g_1^{\text{tot}} + g_3^{\text{tot}})} + \frac{g_4 - \frac{1}{2}(g_3 + g_5)}{g_4^{\text{tot}} - \frac{1}{2}(g_3^{\text{tot}} + g_5^{\text{tot}})} \right] \\ H_{WT}(X_{WT}) &= \frac{1}{2} \left[ \frac{g_8 - \frac{1}{2}(g_7 + g_9)}{g_8^{\text{tot}} - \frac{1}{2}(g_7^{\text{tot}} + g_9^{\text{tot}})} + \frac{g_{10} - \frac{1}{2}(g_9 + g_{11})}{g_{10}^{\text{tot}} - \frac{1}{2}(g_9^{\text{tot}} + g_{11}^{\text{tot}})} \right] \end{aligned}$$

Here,  $r_i$  denotes the integrated red intensity in the upper box labeled  $i$  and  $r_i^{\text{tot}}$  denotes the integrated red intensity in the combined upper and lower boxes labeled  $i$  ( $g_i$  and  $g_i^{\text{tot}}$  are the analogous green intensities).

The ON/OFF ratio for each target ( $\gamma(X_M)$  or  $\gamma(X_{WT})$ ) is calculated for each replicate (Table S4) as:

$$\begin{aligned} \gamma(X_M) &= H_M(X_M)/H_{WT}(X_M), \\ \gamma(X_{WT}) &= H_{WT}(X_{WT})/H_M(X_{WT}). \end{aligned}$$

Here,  $\gamma(X)$  quantifies the ON state of the cascade with the cognate HCR system relative to the OFF state of the cascade with the off-target HCR system (comparing two channels within a single experiment).

\*For BRAF,  $H_M \equiv H^U$  and  $H_{WT} \equiv H^A$ . For JAK2,  $H_M \equiv H^A$  and  $H_{WT} \equiv H^C$ . For PTEN,  $X_M \equiv H^C$  and  $H_{WT} \equiv H^G$ .

†For BRAF,  $X_M \equiv X^A$  and  $X_{WT} \equiv X^U$ . For JAK2,  $X_M \equiv X^U$  and  $X_{WT} \equiv X^G$ . For PTEN,  $X_M \equiv X^G$  and  $X_{WT} \equiv X^C$ .

The ON/OFF ratio for each HCR system ( $\gamma(H_M)$  or  $\gamma(H_{WT})$ ) is calculated for each replicate (Table S5) as:

$$\begin{aligned}\gamma(H_M) &= H_M(X_M)/H_M(X_{WT}), \\ \gamma(H_{WT}) &= H_{WT}(X_{WT})/H_{WT}(X_M).\end{aligned}$$

Here,  $\gamma(H)$  quantifies the ON state of the cascade with the cognate target relative to the OFF state of the cascade with the off-target (comparing a single channel between two experiments).

To characterize the distribution of measurements for a given ON/OFF ratio, we calculate the sample median over five replicates to provide a robust estimate of location (noting that the sample mean is not robust to outliers) and the sample median absolute deviation (MAD):

$$\text{MAD} = \text{median}_j |\gamma_j - \text{median}_j(\gamma_j)|$$

over five replicates to provide a robust estimate of scale (noting that the sample standard deviation is not robust to outliers).<sup>3,4</sup>

**Table S4.** ON/OFF ratio for each target ( $X_M$  or  $X_{WT}$ ) for each of three cancer markers (BRAF, JAK2, PTEN).

	BRAF U1799A		JAK2 G1849U		PTEN C388G	
	$\gamma(X_M)$	$\gamma(X_{WT})$	$\gamma(X_M)$	$\gamma(X_{WT})$	$\gamma(X_M)$	$\gamma(X_{WT})$
Replicate 1	9.9	12.9	50.5	15.3	48.2	46.7
Replicate 2	8.8	15.0	50.4	19.1	71.0	17.9
Replicate 3	14.8	12.9	70.5	14.1	71.1	11.8
Replicate 4	9.8	17.7	20.3	21.0	53.6	28.0
Replicate 5	13.5	22.9	45.7	71.8	95.1	34.0
Median	9.9	15.0	50.4	19.1	71.0	28.0
Median absolute deviation	1.1	2.1	4.7	3.8	17.3	10.1

**Table S5.** ON/OFF ratio for each HCR system ( $H_M$  or  $H_{WT}$ ) for each of three cancer markers (BRAF, JAK2, PTEN).

	BRAF U1799A		JAK2 G1849U		PTEN C388G	
	$\gamma(H_M)$	$\gamma(H_{WT})$	$\gamma(H_M)$	$\gamma(H_{WT})$	$\gamma(H_M)$	$\gamma(H_{WT})$
Replicate 1	10.6	12.0	13.5	56.9	62.2	36.2
Replicate 2	13.1	10.0	16.4	58.6	31.5	40.5
Replicate 3	14.2	13.4	14.1	70.2	30.2	27.7
Replicate 4	14.0	12.3	19.0	22.4	62.7	24.0
Replicate 5	19.6	15.8	63.0	52.1	71.9	44.9
Median	14.0	12.3	16.4	56.9	62.2	36.2
Median absolute deviation	0.9	1.1	2.6	4.7	9.7	8.5



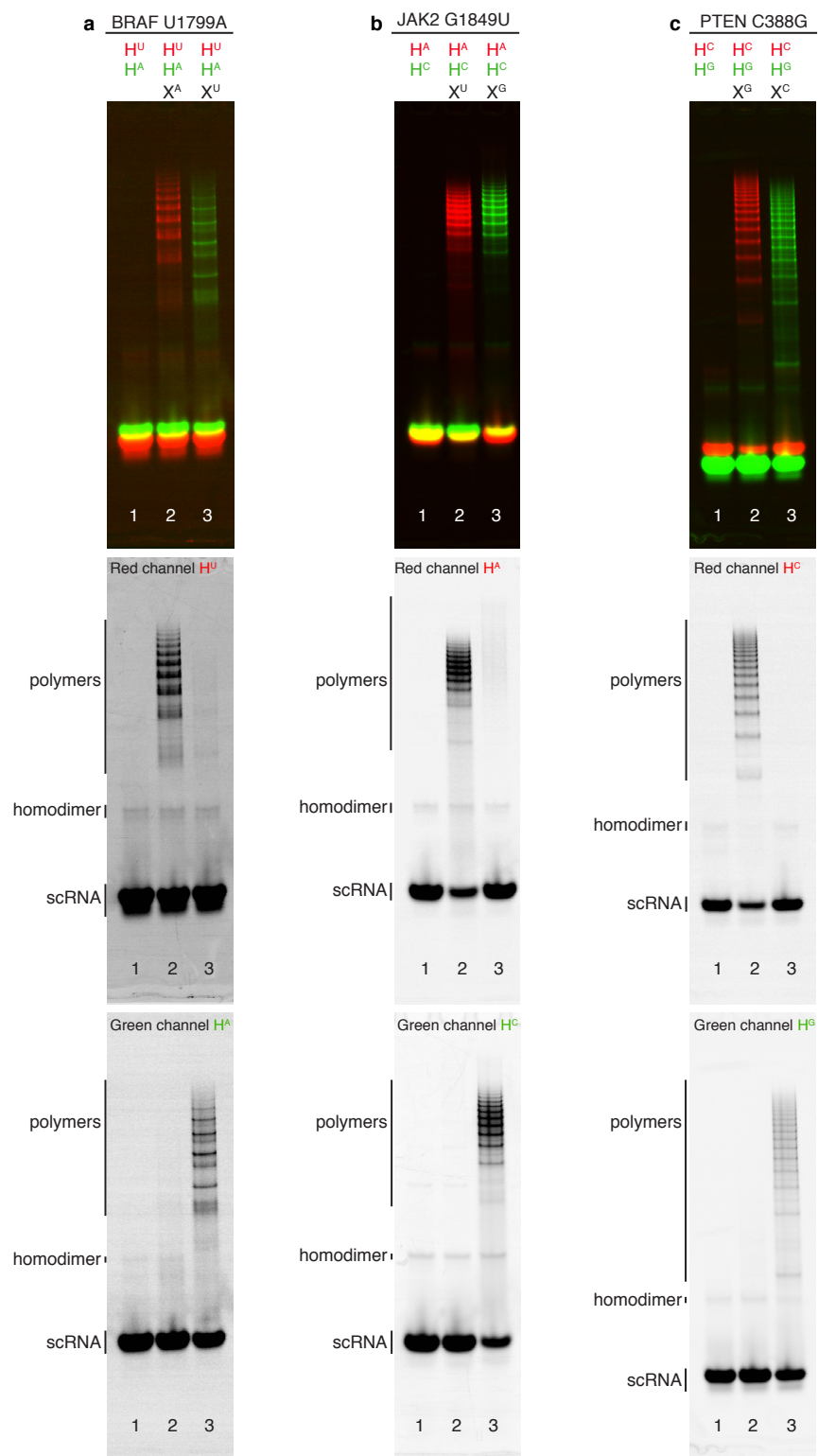


**Figure S1. Annotated single-channel scans for the gels in Figure 3.** Discrimination of RNA SBS cancer markers and wild-type sequences for (a) BRAF U1799A, (b) JAK2 G1849U, and (c) PTEN C388G. Each reaction contains two HCR systems labeled with spectrally distinct fluorophores: one targeting the SBS cancer marker (red channel) and one targeting the corresponding wildtype sequence (green channel). For each HCR system, the fluorophore is carried by one of the two scRNAs (see Table S3). Top: composite image. Middle: red channel. Bottom: green channel.

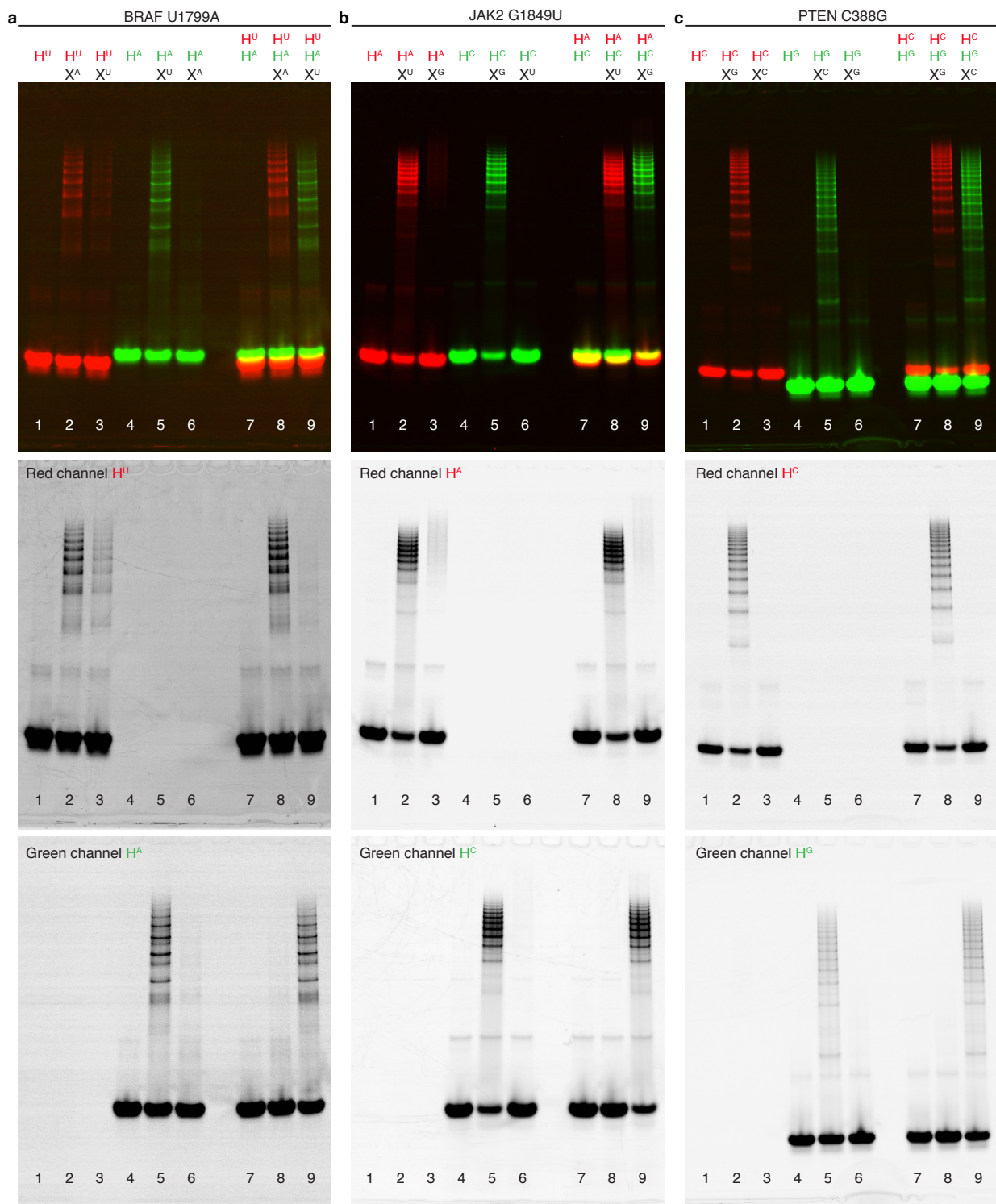


**Figure S2. Further characterization of the scRNAs used in Figure 3.** Discrimination of RNA SBS cancer markers and wildtype sequences for (a) BRAF U1799A, (b) JAK2 G1849U, and (c) PTEN C388G. Each experiment contains a mutant-detecting HCR system (lanes 1–3), a wildtype-detecting HCR system (lanes 4–6), or both HCR systems (lanes 7–9). Top: composite image. Middle: red channel (mutant-detecting HCR systems). Bottom: green channel (wildtype-detecting HCR systems).

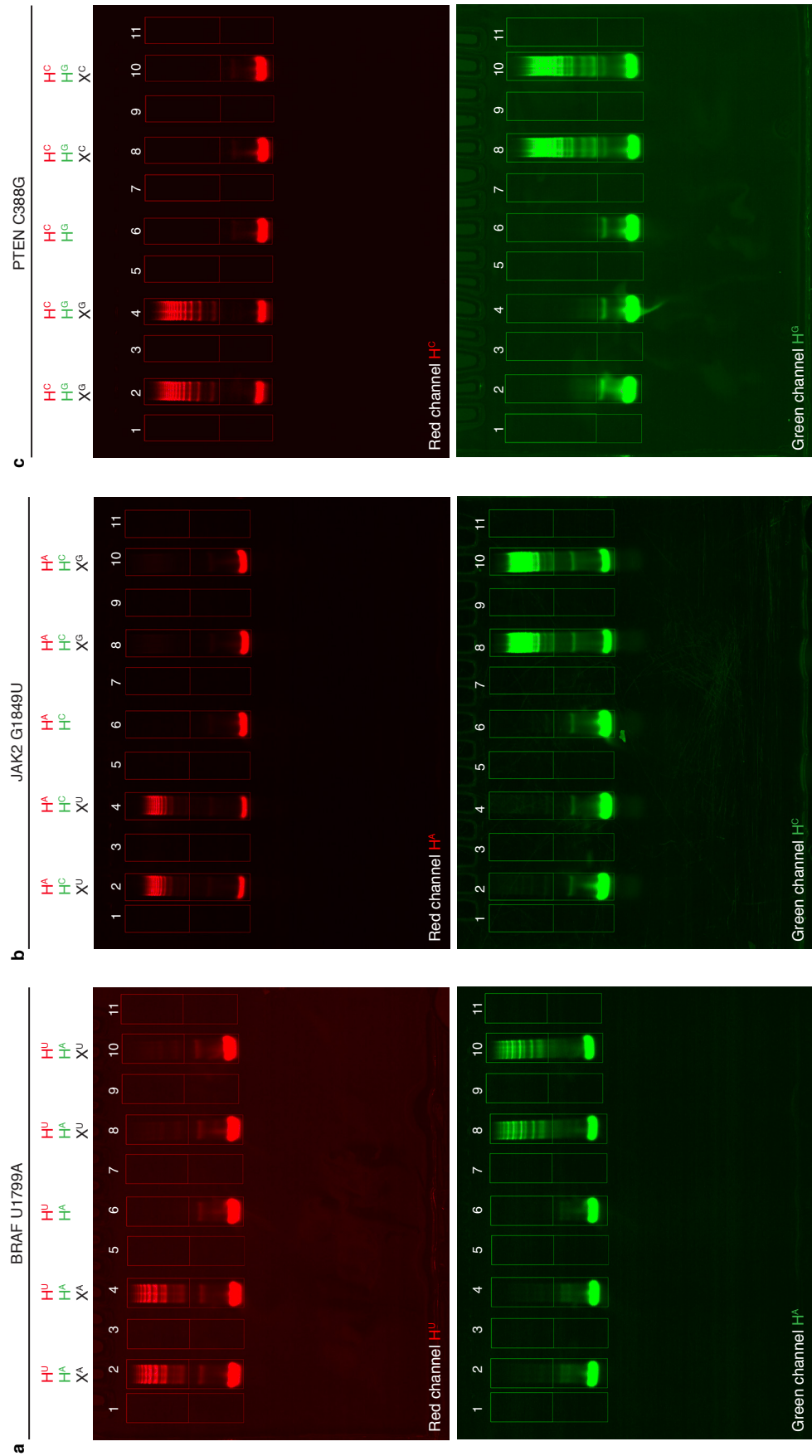


**Figure S3. Quantification of ON and OFF states.** Discrimination of RNA SBS cancer markers and wildtype sequences for (a) BRAF U1799A, (b) JAK2 G1849U, and (c) PTEN C388G. ON and OFF states are quantified using reactions containing both a mutant-detecting HCR system (red channel) and a wildtype-detecting HCR system (green channel) (boxes 2,4,8,10). Gel background is quantified using reactions that contain neither HCR system (boxes 1,3,5,7,9,11). Spontaneous leakage is depicted in box 6.

## S3 Enhancing selectivity via competitive inhibition with an unstructured scavenger

### S3.1 Further characterization of the scRNAs and scavenger used in Figure 4

Figure S4 characterizes the gel migration of reactants and intermediates for the scavenger system used in Figure 4.

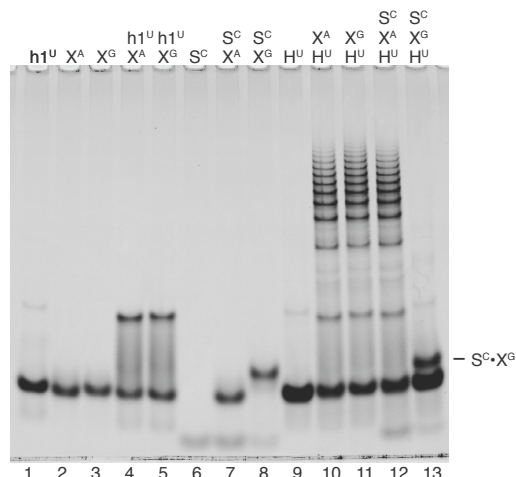


**Figure S4. Enhancing selectivity via competitive inhibition using an unstructured scavenger strand (see Figure 4).** Without scavenger, HCR system  $H^U$  is not selective for cognate target  $X^A$  (forming Watson–Crick pair U·A) over 1-nt sequence variant  $X^G$  (forming nearly isoenergetic wobble pair U·G) (lanes 10 and 11). Scavenger  $S^C$  is selective for  $X^G$ , restoring  $H^U$  selectivity via competitive inhibition (lanes 12 and 13). HCR system  $H^U$  comprises scRNAs  $h1^U$  and  $h2$ .

### S3.2 Scavenger studies with additional SNPs

To explore the general utility of the scavenger concept, we tested six HCR systems (see Table S3) designed to selectively detect the BRAF U1799A, JAK2 G1849U, and PTEN C388G mutant and wildtype sequences against all four possible sequence variants at each mutation position. These 24 case studies (1 cognate target and 3 off-targets for each of six HCR systems) turned up six 1-nt sequence variants that challenged the selectivity of HCR cascades; in each case, HCR selectivity was restored via competitive inhibition by the appropriate scavenger (Figure S5).

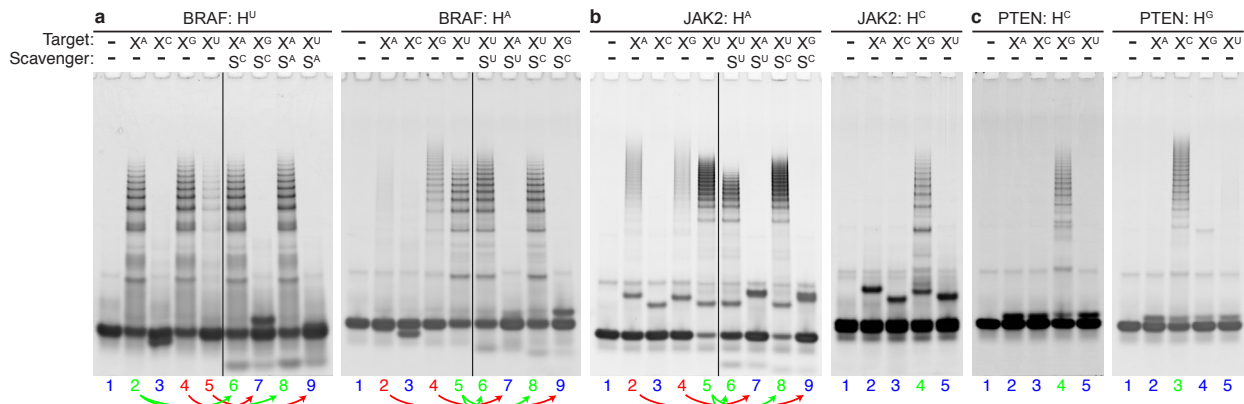


**Figure S5. Scavenger studies with additional SNPs.** For each of three cancer markers, (a) BRAF U1799A, (b) JAK2 G1849U, and (c) PTEN C388G, the selectivity of mutant-detecting and wildtype-detecting HCR systems was tested against all four possible sequence variants (A, C, G, U) at the mutation position. Blue lane numbers denote satisfactory OFF states. Red lane numbers denote suboptimal OFF states in the absence of scavenger, which are converted to satisfactory OFF states using the appropriate scavenger (red arrows to blue lane numbers). Strong ON states are observed with or without scavenger (green lane numbers).

## S4 Genotyping SNPs

### S4.1 Annotated single-channel scans for the gel in Figure 5

Single-channel scans for the gel in Figure 5 are shown in Figure S6, including annotation of scRNAs, homodimers, and polymers for each of four HCR systems.

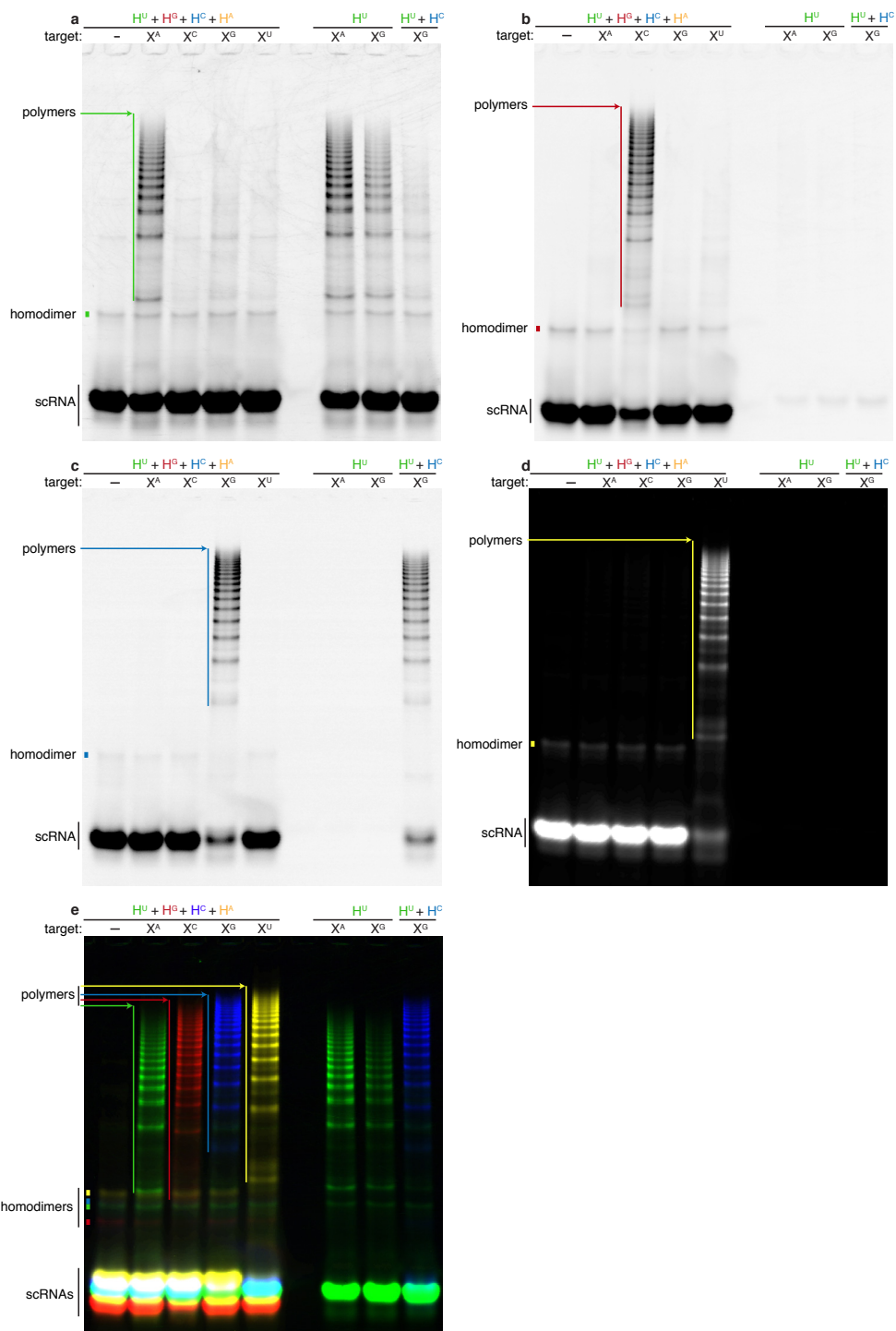


**Figure S6. Annotated single-channel scans for the gel in Figure 5.** (a) Green channel:  $H^U$ . (b) Red channel:  $H^G$ . (c) Blue channel:  $H^C$ . (d) Yellow channel:  $H^A$ . (e) Composite image. For each HCR system, the fluorophore is carried by one of the two scRNAs (see Table S3).

## S5 Additional studies

### S5.1 Effect of SBS mutation location on scRNA selectivity

We were curious whether the location of an SBS mutation with respect to the toehold and stem of an h1 scRNA would affect the selectivity of the conditional hybridization cascade. The studies of Figure S7 did not yield conclusive trends; we include these results to provide a starting point for future work. Based on the evidence obtained to this point, it appears that positioning the SBS mutation so that it hybridizes to the half of the stem near the scRNA toehold (M2 in Figure S7) is as good as or better than positioning the mutation elsewhere.

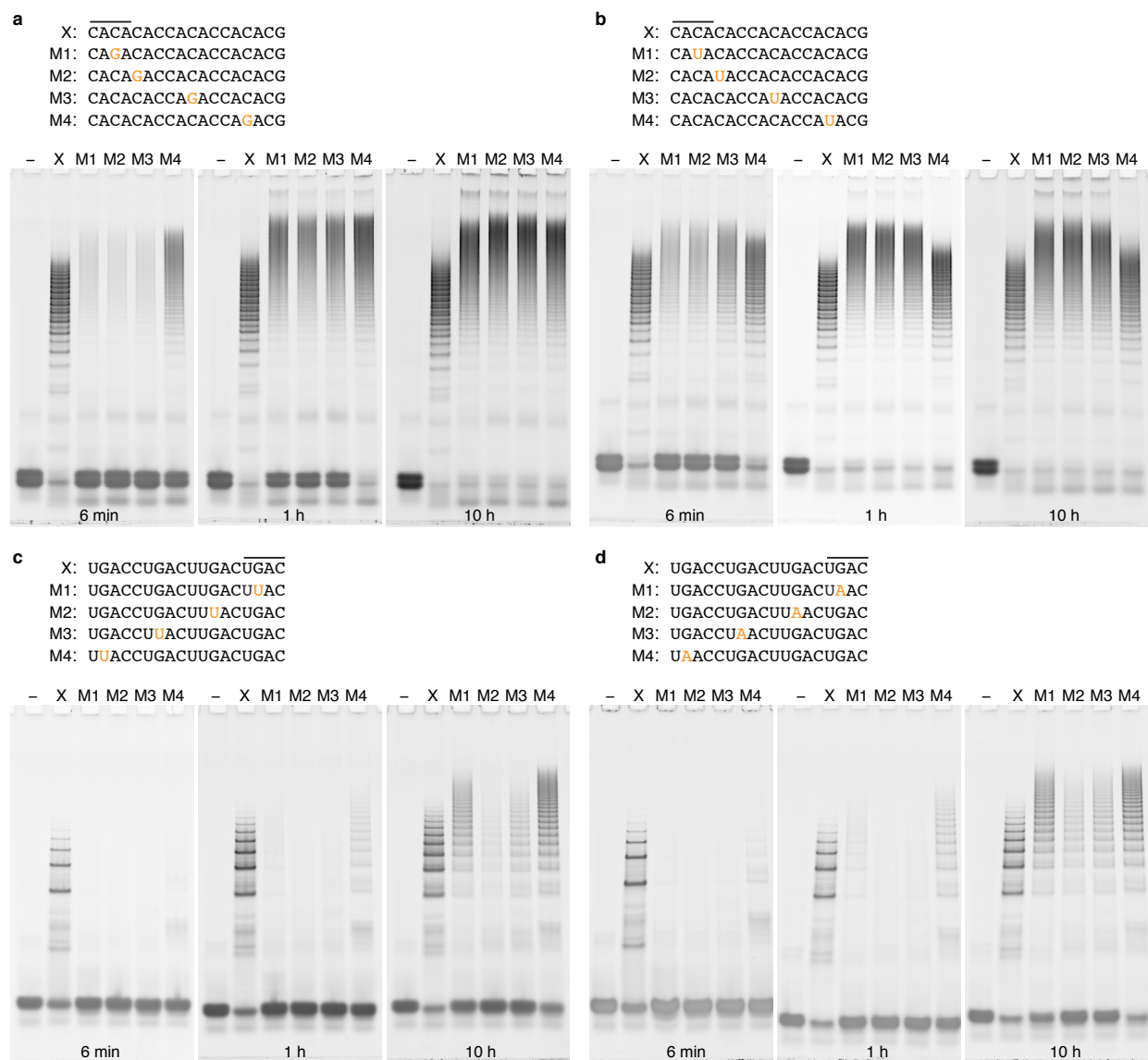


**Figure S7. Effect of SBS mutation location on scRNA selectivity.** For each of two cognate targets, an HCR system was designed to discriminate against two families of 1-nt mismatches. For each family of mismatches, the mutation and nearest neighbors are constant (panel a: ACA→AGA, panel b: ACA→AUA, panel c: UGA→UUA, panel d: UGA→UAA). All targets are predicted to be relatively free of secondary structure. The hybridization site of the toehold of scRNA h1 is noted with a line above the cognate sequence.

## S5.2 Effect of temperature on scRNA selectivity

To examine the effect of temperature on scRNA selectivity, we tested the HCR systems used in Figure 2 ( $H^{\text{fast}}$ ,  $H^{\text{medium}}$ , and  $H^{\text{slow}}$ ) with cognate target X and 1-nt sequence variant  $X'$  over a range of temperatures from 1 °C to 49 °C. Each HCR system exhibits selectivity over a range of temperatures. The timing of the selectivity window shifts to shorter times with increasing temperature and longer times with decreasing temperature. These data demonstrate that 1-nt selectivity can be engineered at a wide range of timescales and temperatures.

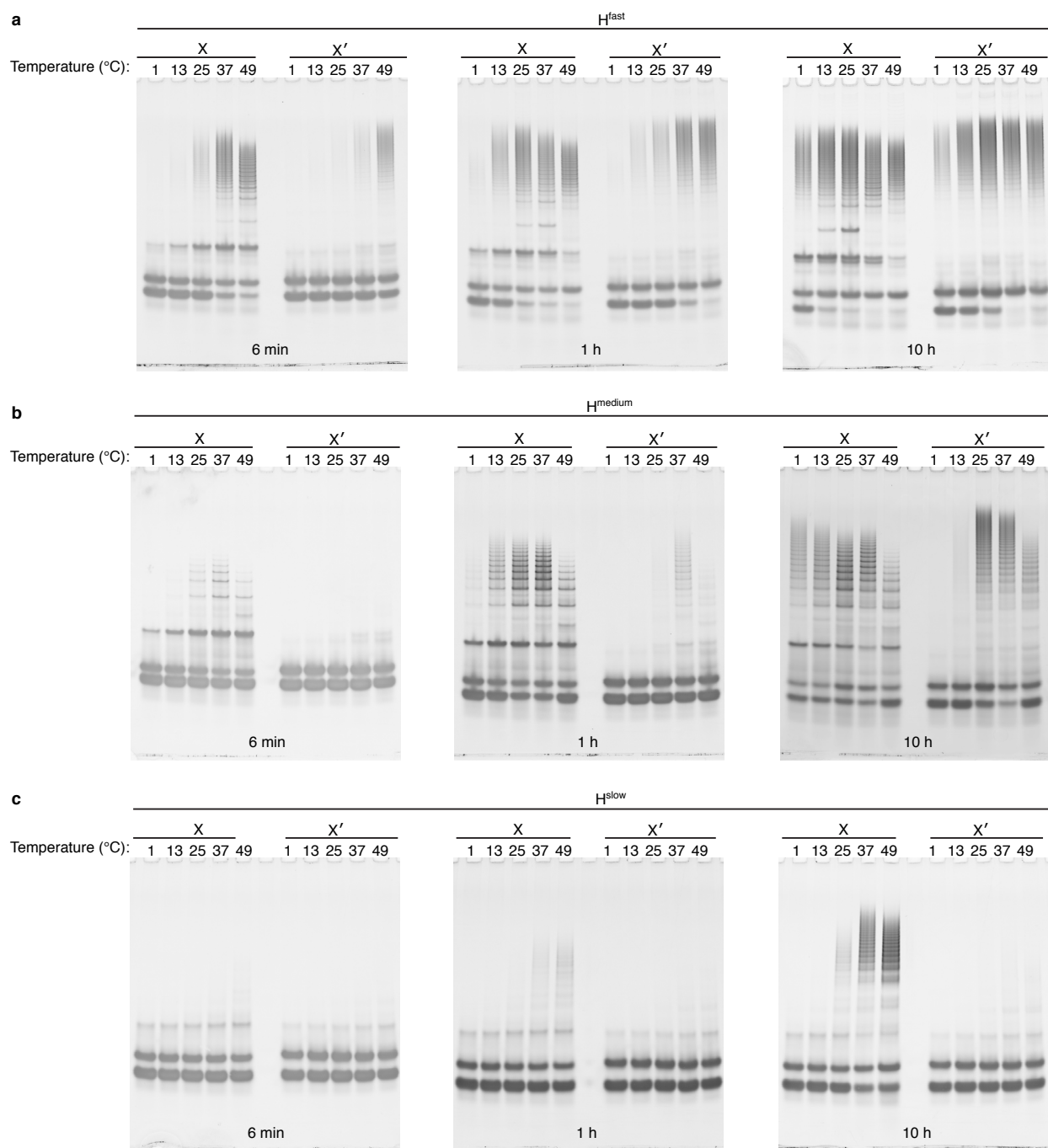


**Figure S8. Effect of temperature on scRNA selectivity.** The HCR systems (a)  $H^{\text{fast}}$ , (b)  $H^{\text{medium}}$ , and (c)  $H^{\text{slow}}$  were tested with cognate target X and 1-nt sequence variant  $X'$  over a range of temperatures from 1 °C to 49 °C.

## References

- (1) Zadeh, J. N.; Steenberg, C. D.; Bois, J. S.; Wolfe, B. R.; Pierce, M. B.; Khan, A. R.; Dirks, R. M.; Pierce, N. A. *J. Comput. Chem.* **2011**, 32, 170–173.
- (2) Choi, H. M. T.; Beck, V. A.; Pierce, N. A. *ACS Nano* **2014**, 8, 4284–4294.
- (3) Maronna, R.; Martin, D.; Yohai, V. *Robust Statistics: Theory and Methods*; Wiley: Chichester, England, 2006.
- (4) Huber, P.J.; Ronchetti, E.M. *Robust Statistics*; Wiley: Hoboken, New Jersey, 2009.